

## Selective Adsorption of CO<sub>2</sub> from Light Gas Mixtures by Using a Structurally Dynamic Porous Coordination Polymer\*\*

Kristi L. Kauffman, Jeffrey T. Culp, Andrew J. Allen, Laura Espinal, Winnie Wong-Ng, Thomas D. Brown, Angela Goodman, Mark P. Bernardo, Russel J. Pancoast, Danielle Chirdon, and Christopher Matranga\*

Gas separations are important to many diverse areas of fossil energy including pre- and post-combustion CO<sub>2</sub> capture and fuel cell applications. The need for efficient gas purification processes has led to interest in adsorption-based separations and new sorbent materials. Porous coordination polymers (PCPs), commonly referred to as metal–organic frameworks (MOFs), lend a great deal of structural versatility to such applications.<sup>[1]</sup> A combination of organic and inorganic building blocks, these multi-dimensional hosts can be tailored for selective adsorption of one guest over another through methods such as pore-size exclusion, mesh-size adjustable sieving, and guest-dependent structural dynamics.<sup>[1,2]</sup>

The numerous reports on structurally dynamic PCPs illustrate the potential of these materials for adsorption applications yet there are only a few reports demonstrating actual gas separations.<sup>[1,3]</sup> A structural breathing phenomenon in the MIL-53 family of MOFs was found to have a significant role in the ability of this sorbent to separate CO<sub>2</sub> and CH<sub>4</sub>.<sup>[3b,4]</sup> Despite the detailed studies of MIL-53, there are currently no

experimental or theoretical methodologies to predict gas selectivities in other structurally dynamic systems or to indicate how generally applicable the MIL-53 separation mechanism may be. Additional studies with actual gas mixtures are needed to advance our theoretical and empirical understanding of structurally dynamic PCPs.

Much of the literature on selective adsorption in PCPs is based on the prediction of a separation extrapolated from pure gas isotherms or calculations from the ideal adsorbed solution theory (IAST), not from actual experimental observations.<sup>[1]</sup> Recent publications point out that the use of IAST to predict selectivities in structurally dynamic PCPs can be complicated by the possibility of cooperative adsorption effects, indicating the need for new fundamental insight into how specific structurally dynamic PCPs selectively adsorb gases.<sup>[1b,5]</sup> While one computational study has investigated the role of stepped isotherms in the separation of CO<sub>2</sub>/N<sub>2</sub> mixtures,<sup>[6]</sup> most models only address single-component adsorption. Recent reviews highlight the lack of fundamental understanding of gas-selective adsorption in these sorbents, indicating the need for experiments and theoretical calculations to shed light on this important phenomenon.<sup>[1]</sup>

Perhaps the most crucial mechanistic issue to address in structurally dynamic systems surrounds what happens to gas interactions with the sorbent before and after the transition between states of differing porosity. The gas- and temperature-dependent threshold pressures ( $P_{th}$ ), above which a rapid rise in gas uptake is noted in most structurally dynamic PCPs, has led many to hypothesize this process could be used to selectively adsorb gases. Yet others have cautioned it could lead to cooperative adsorption where one gas initiates and stabilizes the structural transition, allowing all other gases in the mixture equal access to the open pore network, thus negating the selective aspect of the threshold pressure/temperature.<sup>[1,5]</sup> In short, there is uncertainty in the literature about whether or not the mere presence of a threshold pressure or “gate opening effect” for one gas species at a given pressure/temperature guarantees selectivity over another gas which does not initiate this “gate opening” at the same pressure/temperature. Currently, there are no theoretical or empirical formalisms which can be used to predict when cooperative adsorption may occur.

The data presented here indicates that selectivity results from the structural transition in catena-bis(dibenzoylmethanato)-(4,4'-bipyridyl)nickel(II), referred to as “NiDBM-Bpy” (Figure 1, right, and Figure S1 in the Supporting Information), for the CO<sub>2</sub>, N<sub>2</sub>, and CH<sub>4</sub> mixtures reported here. There

[\*] Dr. K. L. Kauffman, Dr. J. T. Culp, T. D. Brown, Dr. A. Goodman, M. P. Bernardo, R. J. Pancoast, D. Chirdon, Dr. C. Matranga  
National Energy Technology Laboratory, United States Department of Energy  
P.O. Box 10940, Pittsburgh, PA 15236 (USA)  
E-mail: christopher.matranga@netl.doe.gov

Dr. J. T. Culp  
URS, P.O. Box 618, South Park, PA 15129 (USA)  
Dr. A. J. Allen, Dr. L. Espinal, Dr. W. Wong-Ng  
National Institute of Standards and Technology  
United States Department of Commerce  
Gaithersburg, MD 20899 (USA)

[\*\*] This work was performed in support of the National Energy Technology Laboratory's ongoing research in CO<sub>2</sub> capture under the RES contract DE-FE0004000 and has utilized neutron scattering facilities supported in part by the National Science Foundation under Agreement No. DMR-0454672. Reference in this work to any specific commercial product is to facilitate understanding and does not necessarily imply endorsement by the United States Department of Energy. Certain commercial materials and equipment are identified in this paper only to specify adequately the experimental procedure. In no case does such identification imply recommendation by NIST nor does it imply that the material or equipment identified is necessarily the best available for this purpose. The authors thank Juscelino Leao, Wendy Queen, and Craig Brown of the NIST Center for Neutron Research and Martin Green of NIST Ceramics Division for their valuable technical discussions and contributions.

Supporting information for this article is available on the WWW under <http://dx.doi.org/10.1002/anie.201104130>.

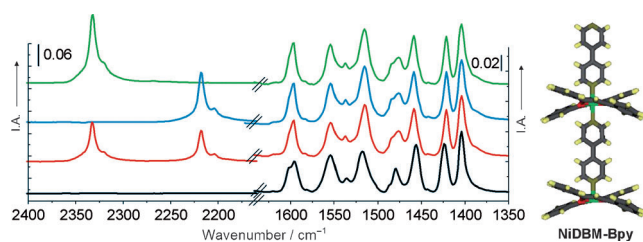


**Figure 1.** Left: Representative spectra of the  $\nu_3$  antisymmetric stretching region ( $2400\text{--}2200\text{ cm}^{-1}$ ) of adsorbed gases and the aromatic bending mode ( $1650\text{--}1350\text{ cm}^{-1}$ ) of NiDBM-Bpy at  $30^\circ\text{C}$  (303 K) and  $P_s$ : vacuum (black), 50/50  $\text{CO}_2/\text{N}_2\text{O}$  (red),  $\text{N}_2\text{O}$  (blue),  $\text{CO}_2$  (green). I.A. = integrated area. Right: A view showing an isolated chain of NiDBM-BPY. C, gray; H, yellow; O, red; N, orange; Ni, green.

appears to be a thermodynamic driving force for the selective inclusion of  $\text{CO}_2$  into NiDBM-Bpy over both  $\text{N}_2$  and  $\text{CH}_4$ . An understanding of the mechanism behind this selectivity will help researchers determine the structural, energetic, and mechanistic reasons for this behavior, thus enabling the development of new dynamic sorbent systems for separation applications.

NiDBM-Bpy was chosen because of its dynamic behavior<sup>[7]</sup> and our previous in situ FTIR investigations show a structural transition accompanies the rapid rise in gas uptake at  $P_{\text{th}}$ .<sup>[8]</sup> In situ FTIR (Supporting Information)<sup>[9]</sup> allows guest and sorbent vibrations to be probed simultaneously (Figure 1). Adsorption isotherms can be generated using the integrated area (I.A.) of the  $\text{CO}_2$  ( $2333\text{ cm}^{-1}$ ) or  $\text{N}_2\text{O}$  ( $2218\text{ cm}^{-1}$ )  $\nu_3$  anti-symmetric mode normalized to characteristic sorbent bands ( $1328\text{--}1650\text{ cm}^{-1}$ ) (Figure 1). In situ IR determined isotherms for 50/50 partial pressure mixtures (red) of  $\text{CO}_2/\text{N}_2$ , and  $\text{CO}_2/\text{CH}_4$  on NiDBM-Bpy as compared to pure  $\text{CO}_2$  isotherms (black) are shown in Figure 2. Observed  $P_{\text{th}}$  values are summarized in Table S1 (Supporting Information).  $\text{CO}_2$  uptake proceeds with a pronounced step beyond  $P_{\text{th}}$  and a large desorption hysteresis for all mixtures studied. For the  $\text{CO}_2/\text{N}_2$  and  $\text{CO}_2/\text{CH}_4$  mixtures, the partial  $\text{CO}_2$  pressure ( $P_{\text{CO}_2}$ ) at  $P_{\text{th}}$  was equivalent to that of pure  $\text{CO}_2$  (Figure 2 a,b), indicating that  $\text{CO}_2$  uptake is a function of  $P_{\text{CO}_2}$  rather than the total pressure ( $P_{\text{tot}}$ ) for these mixtures. Conversely, if the isotherms are plotted as a function of the total pressure, the threshold pressures for these mixtures are roughly double that of pure  $\text{CO}_2$  (Figure 2 c,d and Table S1). Multiple spectra taken at a saturation pressure ( $P_s$ ) where NiDBM-Bpy is saturated with guest molecules, show that the  $\text{CO}_2$  saturation coverage for both the  $\text{CO}_2/\text{N}_2$  and  $\text{CO}_2/\text{CH}_4$  mixtures is identical to what was obtained in pure  $\text{CO}_2$  (Table S2). Because the normalized  $\text{CO}_2$  coverage at saturation in the mixture matches that of pure  $\text{CO}_2$ , we conclude that NiDBM-Bpy preferentially adsorbs  $\text{CO}_2$  over both  $\text{N}_2$  and  $\text{CH}_4$  without displacement of  $\text{CO}_2$ . No significant changes were observed in the position or line shape of the  $\text{CO}_2$   $\nu_3$  asymmetric stretch, indicating the environment for adsorbed  $\text{CO}_2$  is unaltered in the mixture experiments. The fact that  $P_{\text{CO}_2}$  at  $P_{\text{th}}$  is independent of composition for both the  $\text{CO}_2/\text{N}_2$  and  $\text{CO}_2/\text{CH}_4$  mixtures suggests that  $\text{N}_2$  and  $\text{CH}_4$  have little impact initiating or stabilizing the NiDBM-Bpy structural transition at these conditions.

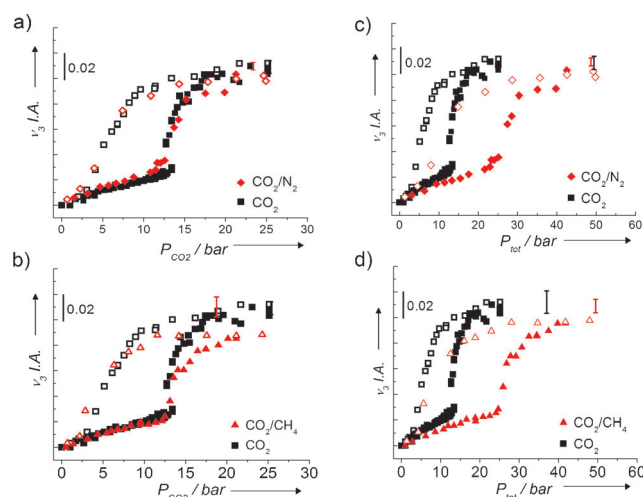


**Figure 2.** IR adsorption (solid) and desorption isotherms (open) at  $30^\circ\text{C}$  (303 K) generated from the normalized integrated area (I.A.) of the  $\text{CO}_2$   $\nu_3$  anti-symmetric stretch for 50/50 binary mixtures of a,c)  $\text{CO}_2/\text{N}_2$  (red diamonds) and b,d)  $\text{CO}_2/\text{CH}_4$  (red triangles) as compared to pure  $\text{CO}_2$  (black squares). Panels (a) and (b) are plotted versus  $\text{CO}_2$  partial pressure ( $P_{\text{CO}_2}$ ), while panels (c) and (d) are plotted versus total pressure ( $P_{\text{tot}}$ ). In this and following figures, the vertical bars represent standard deviation uncertainties ( $N=5$ ) at the saturation pressure ( $P_s$ ).

The IR adsorption isotherm for a 50/50 mixture of  $\text{CO}_2/\text{N}_2\text{O}$  on NiDBM-Bpy at  $30^\circ\text{C}$  (303 K) is shown in Figure 3. The  $\text{CO}_2$   $\nu_3$  band was used to generate the isotherm displayed in Figure 3a while panel b shows the  $\text{N}_2\text{O}$   $\nu_3$  band of the mixture compared to the isotherm of pure  $\text{N}_2\text{O}$  (blue). In contrast to that of pure  $\text{CO}_2$  and  $\text{N}_2\text{O}$ , the normalized saturation coverage from the mixture is significantly less than the pure feed (Table S2). In fact, the integrated intensities at saturation for  $\text{CO}_2$  and  $\text{N}_2\text{O}$  are both approximately half that of their pure gas values. The IR generated isotherms illustrate that both  $\text{CO}_2$  and  $\text{N}_2\text{O}$  coadsorb in this framework in a competitive fashion.  $\text{N}_2\text{O}$  was chosen to test the limits of selectivity in NiDBM-Bpy because it is similar to  $\text{CO}_2$  in size and physical properties. The kinetic diameter of both gases is  $3.3\text{ \AA}$ . The critical temperature for  $\text{N}_2\text{O}$  is  $309.57\text{ K}$  and  $304.14\text{ K}$  for  $\text{CO}_2$  while the boiling point of  $\text{N}_2\text{O}$  is  $-88.5^\circ\text{C}$  ( $184.7\text{ K}$ ) and the sublimation temperature for  $\text{CO}_2$  is

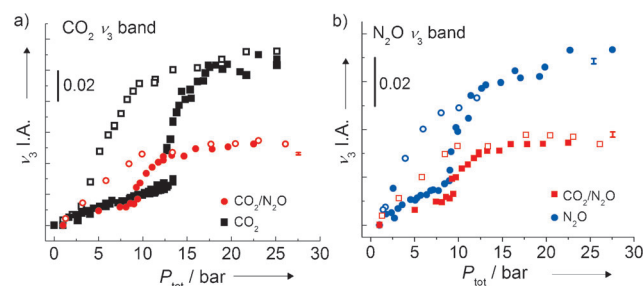


**Figure 3.** IR adsorption (solid) and desorption isotherms (open) at  $30^\circ\text{C}$  (303 K) generated from the normalized integrated area (I.A.) of the a)  $\text{CO}_2$  and b)  $\text{N}_2\text{O}$   $\nu_3$  anti-symmetric mode for a 50/50 mixture of  $\text{CO}_2/\text{N}_2\text{O}$  (red) compared to pure  $\text{CO}_2$  (black squares) and  $\text{N}_2\text{O}$  isotherms (blue circles).

$-78.5^{\circ}\text{C}$  (194.7 K).<sup>[10]</sup> There is also the benefit that  $\text{N}_2\text{O}$  and  $\text{CO}_2$  are both IR active, allowing them to be directly monitored using FTIR (Figure 1). The similarity of interaction thermodynamics with NiDBM-Bpy is reflected in the comparable  $P_{\text{th}}$  of the two gases<sup>[11]</sup> at  $30^{\circ}\text{C}$  (303 K), 9.1 and 12.7 bar for  $\text{N}_2\text{O}$  and  $\text{CO}_2$ , respectively, with a  $P_{\text{th}}$  of 9.4 bar for the 50/50 mixture. In comparison, neither pure  $\text{N}_2$  nor  $\text{CH}_4$  are able to initiate the structure change at  $30^{\circ}\text{C}$  (303 K) in the pressure range studied. However, both  $\text{N}_2$  and  $\text{CH}_4$ <sup>[8]</sup> exhibit favorable interactions with NiDBM-Bpy at lower temperatures as demonstrated by step-shaped isotherms (Figure S4).

Further verification of the selective adsorption noted during in situ IR measurements was established using gas chromatography (GC) of the headspace composition before and after equilibration with the sorbent (Supporting Information). The change in headspace composition after equilibrium with NiDBM-Bpy for 50/50 mixtures of  $\text{CO}_2/\text{N}_2$ ,  $\text{CO}_2/\text{CH}_4$ , and  $\text{CO}_2/\text{N}_2\text{O}$  is shown in Figure 4 (see Table S3). Similar results for 80/20 mixtures are shown in the Supporting Information (Figure S6, Table S4). The amount of  $\text{CO}_2$  in the

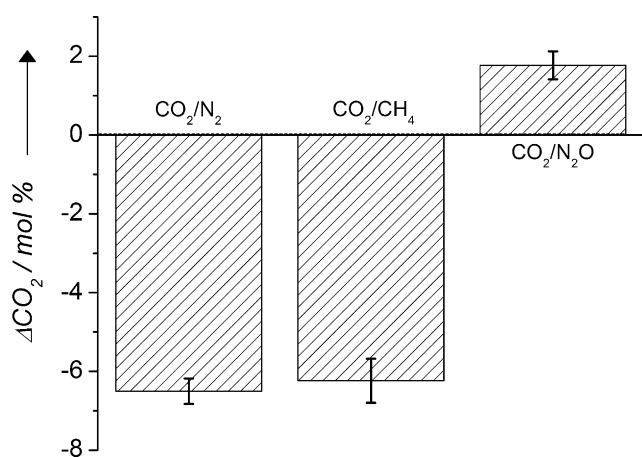


**Figure 4.** The change in mole percent of  $\text{CO}_2$  ( $\Delta\text{CO}_2$ ) in the headspace after equilibrium exposure of gas mixtures (as indicated) to NiDBM-Bpy at  $30^{\circ}\text{C}$  (303 K) and  $P_s$ .

headspace decreased for mixtures of  $\text{CO}_2$  with  $\text{N}_2$  and  $\text{CH}_4$ , indicating preferential adsorption of  $\text{CO}_2$  from the gas phase into the NiDBM-Bpy pore network. Mixtures of 80/20  $\text{CO}_2/\text{CH}_4$  and  $\text{CO}_2/\text{N}_2$  showed complementary decreases in  $\text{CO}_2$  composition. Conversely, changes in the headspace composition were not statistically significant for the 50/50 and 80/20 mixtures of  $\text{CO}_2/\text{N}_2\text{O}$ , confirming the highly competitive adsorption process between  $\text{CO}_2$  and  $\text{N}_2\text{O}$  noted in Figure 3. Results from the GC measurements were in agreement with the predicted equilibrium  $\text{CO}_2$  composition (Table S5) for all three mixtures investigated, further confirming the behavior of this sorbent system.

Representative NiDBM-Bpy vibrational bands under pure gases and mixtures at  $P_s$  are shown in Figure S7. Changes in the NiDBM-Bpy spectrum at 712, 694, 683  $\text{cm}^{-1}$  were observed at pressures above  $P_{\text{th}}$  for both pure gases and mixtures and have been attributed to conformational rearrangements of ligands during the transition to a high porosity

state with an associated adsorption of  $\text{CO}_2$ .<sup>[8a]</sup> Favorable thermodynamics between the guest and the framework help stabilize conformational changes of the dibenzoylmethane (DBM) ligand (see Figure S8), resulting in the observed increase in gas uptake at  $P_{\text{th}}$ .<sup>[8a]</sup> The spectra in Figure S7 indicate the structural transition is independent of gas composition as long as either  $P_{\text{N}_2\text{O}}$  or  $P_{\text{CO}_2}$  is greater than  $P_{\text{th}}$  for  $\text{CO}_2/\text{N}_2$ ,  $\text{CO}_2/\text{CH}_4$ , and  $\text{CO}_2/\text{N}_2\text{O}$  mixtures. In situ FTIR of the NiDBM-Bpy lattice bands illustrate that the ligand environment above  $P_{\text{th}}$  in mixtures of  $\text{CO}_2/\text{N}_2$  and  $\text{CO}_2/\text{CH}_4$  appears unchanged from pure  $\text{CO}_2$  environments, indicating  $\text{CO}_2$  helps stabilize the ligand conformation in the open pore structure.

The lowest-angle (smallest  $Q$ ) diffraction peak, corresponding to the largest  $d$ -spacing in the NiDBM-Bpy structure as indicated in Figure S1, was measured by in situ SANS using the NG3 SANS instrument at the NIST Center for Neutron Research.<sup>[11]</sup> Scattering data were collected on activated NiDBM-Bpy under vacuum, 17 bar of pure  $\text{CO}_2$ , 17 bar of pure  $\text{N}_2$ , and a 50/50 mixture containing 17 bar  $\text{CO}_2$  and 17 bar  $\text{N}_2$  ( $P_{\text{tot}} \approx 34$  bar) at  $30^{\circ}\text{C}$  (303 K) (Figure 5). In the evacuated (guest-free) structure, the  $d$ -spacing was measured

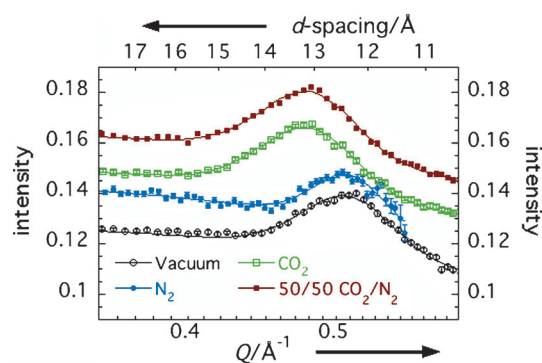


**Figure 5.** SANS diffraction peak data plotted versus both  $Q$  and  $d$ -spacing of NiDBM-Bpy under vacuum (black open circles), 17 bar  $\text{N}_2$  (blue solid circles), 17 bar  $\text{CO}_2$  (green open squares), and a mixture containing 17 bar  $\text{CO}_2$  and 17 bar  $\text{N}_2$  (red solid squares) at  $30^{\circ}\text{C}$  (303 K). Vertical bars are the measurement standard deviation uncertainties for each point.

as  $(12.457 \pm 0.026)$  Å which corresponds to the (002) reflection observed in the X-ray powder diffraction for the guest-free material (Figure S1 and S11). Upon saturation with pure  $\text{CO}_2$  at 17 bar, the  $d$ -spacing shifts to  $(13.284 \pm 0.020)$  Å, confirming the guest-induced structure transition resulting from a lattice expansion. As expected from the IR and GC results, pure  $\text{N}_2$  does not initiate any obvious changes in structure or porosity at 17 bar, yielding a  $d$ -layer spacing of  $(12.364 \pm 0.035)$  Å, which is nearly identical to that obtained for the evacuated structure. Equilibrium adsorption of a 50/50 mixture of  $\text{CO}_2/\text{N}_2$  ( $P_{\text{CO}_2} = 17$ ,  $P_{\text{N}_2} = 17$ , and  $P_{\text{tot}} = 34$  bar) is equivalent to that of pure  $\text{CO}_2$  at 17 bar, further verifying that  $\text{N}_2$  has no effect on the  $\text{CO}_2$ -induced structural transition in NiDBM-Bpy. The in situ SANS data, in combination with the results above, confirm that changes in the lattice spacing and porosity of NiDBM-Bpy brought about by the  $\text{CO}_2/\text{N}_2$

mixture are initiated by CO<sub>2</sub>. Pure N<sub>2</sub> is not capable of initiating or stabilizing a structural transition at these pressures and temperatures. The SANS result for the 50/50 mixture of these gases shows no change from that of pure CO<sub>2</sub>, illustrating that the presence of N<sub>2</sub> in the mixture has no effect on the porosity of the opened NiDBM-Bpy structure. Since the IR data on the ligand vibrations (Figure S7) will be sensitive to both interlayer spacing variations as well as conformational changes, the two sets of data clearly indicate that CO<sub>2</sub> is solely responsible for initiating and stabilizing the equilibrium structure of NiDBM-Bpy in CO<sub>2</sub>/N<sub>2</sub> mixtures when  $P_{\text{CO}_2}$  is in excess of  $P_{\text{th}}$ . Furthermore, the adsorption and separation mechanism involves a lattice expansion in the (002) direction with associated conformational rearrangement of DBM ligands to accommodate the expansion and selective incorporation of CO<sub>2</sub>. This mechanism appears unchanged when comparing pure CO<sub>2</sub> adsorption to that occurring from mixtures.

The guest-dependent phase change and resulting adsorption of gas provides selectivity for CO<sub>2</sub> over N<sub>2</sub> and CH<sub>4</sub>. Volumetric isotherms show pure CO<sub>2</sub>, N<sub>2</sub>, and CH<sub>4</sub> can all initiate and stabilize the phase change, albeit at very different temperatures and pressures. However, CO<sub>2</sub> and N<sub>2</sub>O initiate structural transitions under similar conditions. It is likely the selectivity in this system is driven by the overall thermodynamics of the adsorption process which initiates both the phase change and subsequent uptake of gas. Previous theoretical works by Barrer,<sup>[12]</sup> Coudert,<sup>[4c-e]</sup> and others<sup>[4f,13]</sup> have pointed to the complicated interplay of thermodynamics describing the phase transition, guest-host interactions, stabilizing effects of the guest on the sorbent, relief of mechanical strain in the crystal, and nucleation effects, as being key physical events dictating phase change and gas adsorption conditions in dynamic guest-host systems. We hypothesize that the details of these thermodynamics for each dynamic sorbent system under specific experimental conditions (e.g., temperature, pressure, gas mixture composition) will dictate how efficiently gas separations will occur.

On a final note we stress that the selective adsorption of CO<sub>2</sub> over N<sub>2</sub> and CH<sub>4</sub> in the NiDBM-Bpy system does not imply that all structurally dynamic systems will exhibit similar behavior. As has been pointed out in the literature, the mere presence of a “gate opening effect” or stepped isotherm for one gas species at a pressure/temperature where there is no observation of “gate opening” for another gas, does not imply or guarantee selective adsorption will occur due to the possibility of cooperative adsorption effects.<sup>[1,5]</sup> The systems and conditions where this cooperative adsorption may occur remain unresolved in the literature. Detailed studies of the NiDBM-Bpy system will help unravel the complicated energetics leading to the selective adsorption observed in our work.

Received: June 15, 2011

Revised: August 11, 2011

Published online: September 23, 2011

**Keywords:** IR spectroscopy · metal–organic frameworks · porous coordination polymers · selectivity · structural dynamics

- [1] a) J.-R. Li, R. J. Kuppler, H.-C. Zhou, *Chem. Soc. Rev.* **2009**, *38*, 1477; b) D. M. D’Allesandro, B. Smit, J. R. Long, *Angew. Chem.* **2010**, *122*, 6194; *Angew. Chem. Int. Ed.* **2010**, *49*, 6058.
- [2] a) J.-P. Zhang, S. K. Ghoso, J.-B. Lin, S. Kitagawa, *Inorg. Chem.* **2009**, *48*, 7970; b) S. Q. Ma, D. F. Sun, D. Q. Yuan, X. S. Wang, H. C. Zhou, *J. Am. Chem. Soc.* **2009**, *131*, 6445; c) J. An, R. P. Fliorella, S. J. Geib, N. L. Rosi, *J. Am. Chem. Soc.* **2009**, *131*, 8401; d) B. Wang, A. P. Cote, H. Furukawa, M. O’Keeffe, O. M. Yaghi, *Nature Lett.* **2008**, *453*, 207.
- [3] a) E. Barea, G. Tagliabue, W. G. Wang, M. Perez-Mendoza, L. Mendez-Linan, F. J. Lopez-Garzon, S. Galli, N. Masciocchi, J. A. R. Navarro, *Chem. Eur. J.* **2010**, *16*, 931; b) S. Couck, J. F. M. Denayer, G. V. Baron, T. Remy, J. Gascon, F. Kapteijn, *J. Am. Chem. Soc.* **2009**, *131*, 6326; c) L. Hamon, E. Jolimaire, G. D. Pirngruber, *Ind. Eng. Chem. Res.* **2010**, *49*, 7497; d) K. Nakagawa, D. Tanaka, S. Horike, S. Shimomura, M. Higuchi, S. Kitagawa, *Chem. Commun.* **2010**, *46*, 4258; e) D. Britt, H. Furukawa, B. Wang, T. G. Glover, O. M. Yaghi, *Proc. Natl. Acad. Sci. USA* **2009**, *106*, 20637; f) H. Kanoh, A. Kondo, H. Noguchi, H. Kajiro, A. Tohdoh, Y. Hattori, W. C. Xu, M. Moue, T. Sugiura, K. Morita, H. Tanaka, T. Ohba, K. Kaneko, *J. Colloid Interface Sci.* **2009**, *334*, 1.
- [4] a) L. Hamon, P. L. Llewellyn, T. Devic, A. Ghoufi, G. Clet, V. Cuillerm, G. D. Pirngruber, G. Maurin, C. Serre, G. Dirver, W. van Beek, W. Jolimaire, A. Vimont, M. Daturi, G. J. Ferey, *J. Am. Chem. Soc.* **2009**, *131*, 17490; b) V. Finsy, L. Ma, L. Alaerts, D. E. De Vos, G. V. Baron, J. F. M. Denayer, *Microporous Mesoporous Mater.* **2009**, *120*, 221; c) F.-X. Coudert, M. Jeffroy, A. H. Fuchs, A. Boutin, C. Mellot-Draznieks, *J. Am. Chem. Soc.* **2008**, *130*, 14294; d) F.-X. Coudert, C. Mellot-Draznieks, A. H. Fuchs, A. Boutin, *J. Am. Chem. Soc.* **2009**, *131*, 3442; e) F.-X. Coudert, C. Mellot-Draznieks, A. H. Fuchs, A. Boutin, *J. Am. Chem. Soc.* **2009**, *131*, 11329; f) E. Stavitski, E. A. Pidko, S. Couck, T. Remy, E. J. M. Hensen, B. M. Weckhuysen, J. Denayer, J. Gascon, F. Kapteijn, *Langmuir* **2011**, *27*, 3970.
- [5] Z. R. Herm, J. A. Swisher, B. Smit, R. Krishna, J. R. Long, *J. Am. Chem. Soc.* **2011**, *133*, 5664.
- [6] Q. Y. Yang, L. Ma, C. L. Zhong, X. An, D. Liu, *J. Phys. Chem. C* **2011**, *115*, 2790.
- [7] a) D. V. Soldatov, *J. Inclusion Phenom. Macrocyclic Chem.* **2004**, *48*, 3; b) D. V. Soldatov, G. D. Enright, C. I. Ratcliffe, A. T. Henegouwen, J. A. Ripmeester, *Chem. Mater.* **2001**, *13*, 4322; c) D. V. Soldatov, G. D. Enright, J. A. Ripmeester, *Chem. Mater.* **2002**, *14*, 348; d) D. V. Soldatov, G. D. Enright, J. A. Ripmeester, *Cryst. Growth Des.* **2004**, *4*, 1185; e) D. V. Soldatov, I. L. Moudrakovski, C. I. Ratcliffe, R. Dutrisac, J. A. Ripmeester, *Chem. Mater.* **2003**, *15*, 4180; f) D. V. Soldatov, E. A. Ukraintseva, V. A. Longvinenko, *Struct. Chem.* **2007**, *48*, 938; g) D. V. Soldatov, J. A. Ripmeester, *Mendeleev Commun.* **2004**, *3*, 1.
- [8] a) J. T. Culp, A. L. Goodman, D. Chirdon, S. G. Sankar, C. Matranga, *J. Phys. Chem. C* **2010**, *114*, 2184; b) J. T. Culp, M. R. Smith, E. Bittner, B. Bockrath, *J. Am. Chem. Soc.* **2008**, *130*, 12427.
- [9] a) P. D. C. Dietzel, R. E. Johnsen, H. Fjellvag, S. Bordiga, E. Groppo, S. Chavan, R. Blom, *Chem. Commun.* **2008**, 5125; b) S. Natesakhawat, J. T. Culp, C. Matranga, B. Bockrath, *J. Phys. Chem. C* **2007**, *111*, 1055; c) A. L. Goodman, L. A. Campus, K. T. Schroeder, *Energy Fuels* **2005**, *19*, 471; d) S. G. Kazarian, M. F. Vincent, F. V. Bright, C. L. Liotta, C. A. Eckert, *J. Am. Chem. Soc.* **1996**, *118*, 1729; e) M. R. Nelson, R. F. Borkman, *J. Phys. Chem. A* **1998**, *102*, 7860; f) S. P. Nalawade, F. Picchioni, L. Janssen, D. W. Grijpma, J. Feijen, *J. Appl. Polym. Sci.* **2008**, *109*, 3376; g) C. Serre, S. Bourrelly, A. Vimont, N. A. Ramsahye, G. Maurin, P. L. Llewellyn, M. Daturi, Y. Filinchuk, O. Leynaud, P. Barnes, G. Férey, *Adv. Mater.* **2007**, *19*, 2246; h) A. Vimont, A. Travert, P. Bazin, J. C. Lavalley, M. Daturi, C. Serre, G. Férey, S.

- Bourrelly, P. L. Llewellyn, *Chem. Commun.* **2007**, 3291; i) L. Heinke, D. Tzoulaki, C. Chmelik, F. Hibbe, B. J. M. van, H. Lim, J. Li, R. Krishna, J. Karger, *Phys. Rev. Lett.* **2009**, *102*, 065901.
- [10] D. R. Lide, *Handbook of Chemistry and Physics*, 74 ed., CRC, Ann Arbor, **1994**.
- [11] C. J. Glinka, J. G. Barker, B. Hammouda, S. Kreuger, J. J. Moyer, W. J. Orts, *J. Appl. Crystallogr.* **1998**, *31*, 430.
- [12] a) R. M. Barrer, *J. Phys. Chem. Solids* **1960**, *16*, 84; b) R. M. Barrer, *Philos. Trans. R. Soc. London Ser. A* **1984**, *311*, 333; c) R. M. Barrer, *Pure Appl. Chem.* **1989**, *61*, 1903.
- [13] a) F. Salles, G. Maurin, C. Serre, P. L. Llewellyn, C. Knöfel, H. J. Choi, Y. Filinchuk, L. Oliviero, A. Vimont, J. R. Long, G. Férey, *J. Am. Chem. Soc.* **2010**, *132*, 13782; b) D. Fairen-Jimenez, N. A. Seaton, T. Düren, *Langmuir* **2010**, *26*, 14694; c) A. V. Neimark, F.-X. Coudert, A. Boutin, A. H. Fuchs, *J. Phys. Chem. Lett.* **2010**, *1*, 445; d) A. Ghoufi, G. Maurin, *J. Phys. Chem. C* **2010**, *114*, 6496; e) A. Ghoufi, G. Maurin, G. Férey, *J. Phys. Chem. Lett.* **2010**, *1*, 2810.
-